Efficient Numerical Predictions of MEMS Fluid-Structure Interaction Damping

Jari Hyvärinen* and Jan Söderkvist**
*Anker-Zemer Engineering AB, P.O. Box 156, SE-691 23 Karlskoga, Sweden, jari.h@anker-zemer.se
**Colibri Pro Development AB, Torgnyvägen 48, SE-187 76 Täby, Sweden, js@colibri.se

SUMMARY

The new software LINFLOW is used to look into the fluid-structure (aeroelastic) interaction for MEMS-scaled dimensions. Both fluids in narrow regions and structures surrounded by fluids are addressed. The results are compared with experiments and publications. It is shown that the chosen approach can, without loss of accuracy, reduce the CPU time with more than a factor 100 over conventional simulation programs such as FLOTRAN. That both inertial and viscous effects, as well as some non-linear effects, are accounted for 3-dimensionally results in more reliable results than those obtained via analytic approximations.

Keywords: aeroelasticity, fluid-structure interaction, simulations

INTRODUCTION

Many MEMS devices rely on the interaction between fluids and solids. This is especially noticeable in 'hot' MEMS applications such as medical and biochemical devices (drug delivery systems, lab-on-chip, etc) and IT components (inkjet printers, hard disk drives, etc) [1].

When optimizing the design it is important to consider the general characteristics of this fluid-structure interaction. The complexity of the Navier-Stokes equations makes a detailed analysis of this aeroelastic interaction out of reach for most MEMS persons. The alternatives have been very resource-demanding computer simulations or crude analytic approximations, e.g. Reynolds equation.

New software packages are emerging that enable the study of aeroelasticity on ordinary PCs in a very CPU-efficient manner. This presentation focuses on one of the more promising – a combination of boundary (LINFLOW, version 1.2a) and finite (e.g. ANSYS) element techniques [2].

NUMERICAL APPROACH

Normal flow can be characterized via five unknowns (density ρ, pressure p, velocity vector $\bar{V}$) that can be calculated from the Navier-Stokes equations, the mass conservation, and the isentropic relation for fluids.

LINFLOW initially assumes inviscid (viscosity μ=0) and irrotational flow (non-turbulent, $\nabla\times\bar{V}=0$). The velocity potential Φ ($\bar{V}=\nabla\Phi$) can then be introduced which gives the following two key equations [3]:

$$\nabla^2\Phi-\left(\frac{U_\infty}{a}\right)^2\cdot\left(\frac{1}{U_\infty}\frac{\partial}{\partial t}+\nabla\right)^2\Phi=0 \qquad (1)$$

$$p=p_\infty+\rho\cdot\left(\frac{U_\infty^2}{2}-\left(\frac{|\bar{v}|^2}{2}+\frac{\partial\Phi}{\partial t}\right)\right) \qquad (2)$$

where a denotes the speed of sound ($a^2=\mathrm{d}p/\mathrm{d}\rho$) and U_∞ the far field free-stream part of $\bar{V}$. Note that incompressible flow ($\mathrm{d}\rho/\mathrm{d}p=0$ → $\nabla^2\Phi=0$) and the acoustic equation (harmonic Φ, frequency f, small perturbations → $\nabla^2\Phi+(2\pi f/a)^2\Phi=0$) are two special cases of eq. (1). The integral formulation of eq. (2) is best solved using the boundary element method.

Furthermore, the un-steady flow is described via harmonic oscillations around some general equilibrium point. This procedure of variable separation and eigenmode decomposition resembles closely that used when solving complicated, general differential equations analytically. Normally, highly accurate solutions are obtained even when using a very limited number of eigenmodes. In our case, ANSYS is used to determine the mechanical fluid-free eigenmodes that are used as input to the fluid-structure interaction problem solved by LINFLOW. The result is a fast, non-iterative, solution procedure for aeroelasticity.

Neglecting viscous effects is well motivated for most macro-scaled devices. However, the viscous shear losses in the boundary layer near the walls cannot be neglected for MEMS-scaled dimensions. The thickness δ_ν of this layer is approximately $(\nu/\pi f)^{1/2}$, where ν ($=\mu/\rho$) is the kinematic viscosity [4]. Special cases are the squeeze-film [5,6] and slide-film [7] damping encountered in many vibrating MEMS-devices. LINFLOW handles viscous effects via additions to its governing set of equations. This enables addressing viscous effects at the same time as inertial (e.g. mass loading) and some non-linear effects. It creates opportunities that go well beyond the analytic approximations normally used in the MEMS community.

FLUIDS IN NARROW REGIONS

The performance of MEMS devices with movable parts is often affected by a fluid-structure interaction. Typical examples include accelerometers (mechanical damping is tailored via fluid-interaction) and pumps. Most such devices include fluids in narrow regions whose thickness often are comparable or smaller than the shear boundary layer δ_v. The viscous shear losses will therefore dominate for enclosed MEMS regions, especially since their fluid flow is parallel to the surfaces.

To predict the fluid damping analytically for such regions is feasible only for very simple geometries. Even for such a simple geometry as the interaction between two comb-finger, one has to apply various approximations such as Couette flow and Stokes type models, with uncertainty in the results as a consequence [7]. Contrary to the analytic approach, the presented simulation procedure is quick and accurate for fluids in narrow regions also for more general geometries. As an illustration, this procedure is applied to some common MEMS geometries with squeeze-film damping.

The first example is two circulate plates, with radius R, separated a distance h_o, that vibrate towards each other. Assume initially that the motion is so slow that inertial effects are negligible. This case has an analytic approximation for the pressure p at radius r:

$$p(r) = p_{external} + 3\mu \cdot \frac{dh_o}{dt} \cdot \frac{R^2 - r^2}{h_o^3} \qquad (3)$$

Results for typical MEMS-scaled dimensions are listed in Table 1. The agreement is excellent for $h_o/R<<1$. Several assumptions made for the analytic approximation fail for larger gaps. For example, the pressure will no longer be constant in the thickness direction, and the edge effects at the plate's periphery are no longer negligible. In fact, the movable plate will 'see' the edge and the surrounding fluid more than the fixed plate, and the pressure distribution near the two plates can differ noticeably, when $h_o>R$.

Table 1: *The pressure increase at the center of two circular plates (R=500 μm) vibrating in air at 1 kHz with an amplitude of $h_o/100$.*

h_o [μm]	*p(0)* [Pa] via LINFLOW	*p(0)* [Pa] via eq. (3)	Ratio
1	861	848	1.01
3	95.0	94.2	1.01
10	8.40	8.48	0.99
30	0.936	0.942	0.99
100	0.0927	0.0848	1.09
300	0.106	0.00942	11.27
1000	0.0684	0.000848	80.66

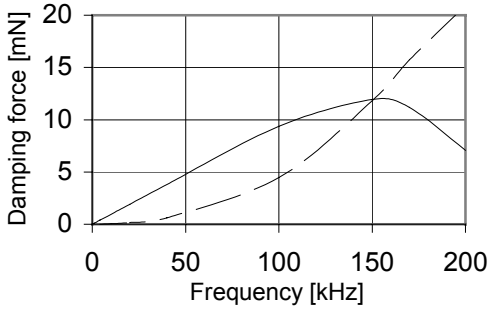

Fig. 1: *The LINFLOW-computed frequency dependence of the real (dashed) and imaginary (solid) part of the reaction force for the 3 μm gap in Table 1.*

Figure 1 shows the behavior at higher frequencies. The reaction force's component out-of-phase with the deflection dominates at low frequencies, leading to energy dissipation. At high frequencies the inertia prevents fluid flow. This reduces viscous damping and results in an elastic Hooke's law governed behavior. The in-phase component, which depends only of ρ, takes over. This case is harder to analyze analytically.

An even more complicated case analytically is rectangular plates with holes. Here, a manageable analytic solution exists only in the absence of holes and with prescribed edge pressures. Assume two 80×80 μm^2 plates in air separated 2 μm, with one of the plates oscillating at 4,580 Hz. Let Hn denote the case where one of the plates contains n^2 holes each covering 1% of the plate area. A typical pressure distribution is illustrated in Fig. 2. The resulting out-of-phase reaction force was compared with $F_{damp}=0.422\cdot\mu\cdot L^4/h_o^3\cdot dh_o/dt$ (L=side length) for H0 [8], and with FLOTRAN results for H0-H2 (Table 2). The comparison was not extended beyond four holes as the CPU-time for FLOTRAN was a limiting factor (see Table 4 in the discussion).

The difference in results in Table 2 is due to FLOTRAN and the analytic expression prescribing the pressure at the plates' and holes' edges. LINFLOW, due to its boundary element formulation, does not require such boundary conditions and accounts automatically for the pressure increase outside edges and holes that occurs is reality, and that would have required an even larger FLOTRAN model to catch.

Table 2: *Damping force [μN] for typical rectangular membranes containing holes.*

Model	LINFLOW	FLOTRAN	Analytic
H0	0.030	0.023	0.022
H1	0.028	0.014	-
H2	0.024	0.0058	-

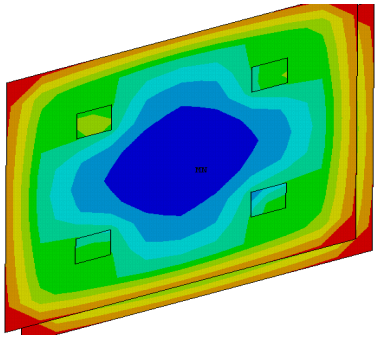

Fig. 2: *LINFLOW pressure results for H2 (four holes).*

FLUID-SURROUNDED STRUCTURES

The most successful MEMS component is the quartz tuning fork watch crystal. It is a suitable example of a small device surrounded by a fluid. Its high frequency stability necessitates its energy losses to be small, i.e. a high Q is needed. Despite it being a simple problem to pose, it is hard to accurately predict Q and its dependence on various parameters. The procedure used in this article offers interesting possibilities.

Measurements on watch crystals' resonant peaks will unveil the surrounding fluid's influence since the mounting and intrinsic losses are low. Such measurements have been performed on commercially available watch crystals from several suppliers (Table 3) having, typically, Q>100,000 and f_o=32.8 kHz in vacuum. The visibility of the very weak liquid-damped resonant peaks was enhanced by compensating for the dielectric capacitance electrically.

The frequency shift, Δf, depends almost linearly on the fluid's density, and only to a minor degree on its viscosity, as seen in Fig. 3a. Thus, fluid mass loading is the important ingredient of Δf in this frequency range. The predictions in table 3 for the frequency shift agree well with the measurements.

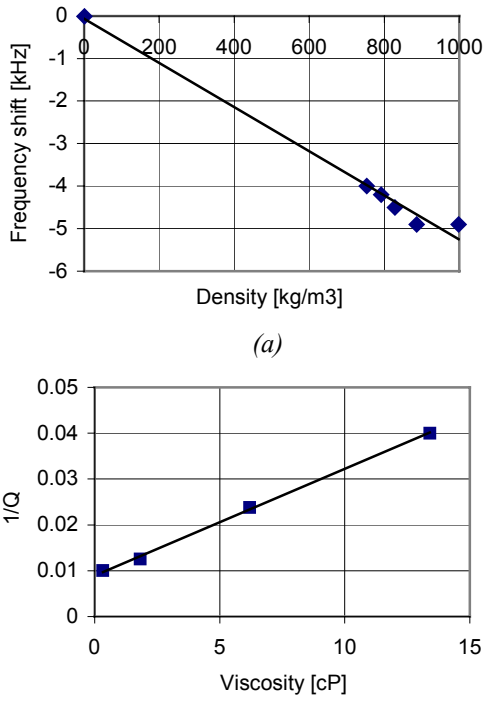

Fig. 3: *Measurement data from Table 3.*

Q depends almost linearly on the viscosity if the density is constant, as seen in Fig. 3b in which only the fluids with roughly the same density has been included. This stresses the importance of the boundary layer δ_v (11 µm in air and 3.1 µm in water). Extrapolating the data shows that Q≈100 can be expected if the viscosity of these liquids had been zero, which agrees well with the Q-predictions in Table 3 for inviscid flow, i.e. with only acoustic losses (Fig. 4).

The influence from the sound velocity, a, is small since the tine velocity is small compared to a.

Table 3: *Data for tested tuning fork watch crystals in various fluids (at room temperature).*

Surrounding fluid	Measured					Predicted	
	ρ [kg/m^3]	μ [cP]	a [m/s]	Δf [kHz]	Q	Δf [kHz]	Q
Air	1.3	0.017	340	-0.0085	12,000	-0.0076	12,500
Acetone	792	0.33	1166	-4.2	100	-4.03	107*
Distilled water	998	1.0	1480	-4.9	(40)**	-4.85	90*
Lamp oil (T-Gul)	753	1.8	1274	-4.0	80	-3.86	111*
Exxsol D140	828	6.2	1372	-4.5	40	-4.18	104*
Pigment-free ink	886	13.4	1402	-4.9	25	-4.41	98*

**) These simulations were made with inviscid flow, as the results were not sufficiently accurate (according to the authors) with viscous effects included. The viscous representation for submerged structures will be updated in LINFLOW's next release.*

***) The accuracy of this value is poor due to that the water's low resistivity hides the resonant peak.*

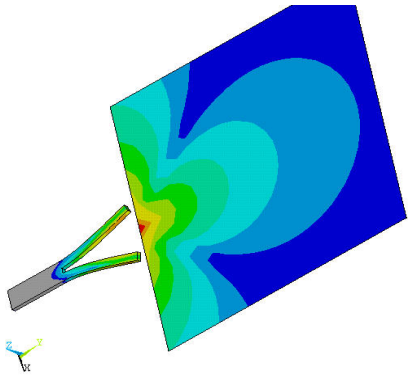

Fig. 4: *The acoustic dipole pressure field on the surface of a MEMS tuning fork and in an arbitrarily located external plane.*

The fluid's influence was analyzed over temperature for Exxsol D140. The results followed the temperature dependence of the material parameters well, e.g. the strong temperature dependence of the viscosity could be seen (10 cP at 5°C and 3.1 cP at 50°C).

In addition, the predicted pressure dependence of the frequency was shown earlier to also agree with reality (see e.g. Fig. 6 in Ref. [3]).

The deviation between measured and predicted Δf and inviscid Q are well within the level of how accurately the dimensions of the tuning forks were measured. Note that the classical expression for how the frequency depends on Q ($f \propto \{1-1/(2Q^2)\}^{1/2}$) is incomplete as it neglects mass-loading.

Interesting to note that asymmetric resonant peaks were observed when the fluid damping forced eigenmodes to be close to each other. Simulations verify this behavior, and show that Q can have a non-trivial frequency dependence near resonant peaks since the fluid's influence on different eigenmodes vary.

DISCUSSION

The presented simulation approach is shown to be an interesting and rapid solution procedure that has great promise. It has been tested and shown to be applicable to a wide range of geometry types and fluids. Some of the more illustrative cases have been included is this article as examples. Ongoing modifications to the viscous implementation will improve the possibilities even further.

Table 4: *Elapsed time for the solution phase.*

Model	**LINFLOW** (Pentium II 266 MHz PC notebook)		**FLOTRAN** (Origin 2000 UNIX server)	
	Time [s]	**nodes**	**Time [s]**	**nodes**
H0	2	242	1650	2,650
H2	135	1,214	9925	15,000

The approach can be very time-efficient when compared with conventional simulation programs (see e.g. Table 4). This enables a more interactive design optimization. The CPU-efficiency, which does not compromise the accuracy, is due to that LINFLOW …

… handles the interaction between mechanical deformations and the fluid's pressure field in a non-iterative way.

… uses the boundary element instead of the finite element method, i.e. fewer elements are needed to handle large structural deformations and geometries with high aspect ratios.

… solves the problem in the frequency domain. Had vibrating MEMS-devices with low energy losses (high Q) instead been addressed in the time domain instead, than a very large number of time steps would have been required to catch the harmonic steady state.

ACKNOWLEDGMENTS

We greatly acknowledge Deepak Ganjoo at Ansys, Inc. for the original H0-H2 FLOTRAN models, and William Day, Mats Ottosson and Ulf Rockström at XaarJet AB for providing liquids and their material parameters.

REFERENCES

[1] Market Analysis for Microsystems 1996-2002, Nexus Office c/o FhG-ISiT, 1998.

[2] www.linflow.com and www.ansys.com

[3] J. Hyvärinen and J. Söderkvist, "Aeroelasticity – The Interplay Between Fluids and Solids", *Accepted for publication in J. Micromech. Microeng.*, **11** (2001).

[4] M. Christen, "Air and Gas Damping of Quartz Tuning Forks, *Sensors and Actuators*, **4** (1983) 555-564.

[5] J.B. Starr, "Squeeze-Film Damping in Solid-State Accelerometers", *Proc. IEEE Solid-State Sensor and Actuator Workshop*, Hilton Head Island, SC, U.S.A., IEEE: 90CH2783-9 (1990) 44-47.

[6] T. Veijola, H. Kuisma, J. Lahdenperä and T. Ryhänen, "Equivalent-Circuit Model of the Squeezed Gas Film in a Silicon Accelerometer", *Sensors and Actuators A* **48** (1995) 239-248.

[7] Y.-H. Cho, A.P. Pisano and R.T. Howe, "Viscous Damping Model for Laterally Oscillating Microstructures", *J. MEMS*, **3**(2) (1994) 81-87.

[8] D. Ganjoo, "ALE for CFD @5.7", *Presented at the 9th Int. Ansys Conf.*, Pittsburgh, USA Aug. 27-30, 2000.